Topographical criteria for the occurrence of landslides causing debris flows in the 2017 torrential rain in northern Kyushu, Japan

Takehiro Ohta[1*], *Kanako* Hamamoto[1,2], and *Seiya* Eguchi[1,3]

[1]Yamaguchi University, Yoshida 1677-1, Yamaguchi, Japan
[2]NEXCO-West Consultants Company Limited, Higashi-ku Futaba-no-sato 3-5-7, Hiroshima, Japan
[3]Kyusyu Electric Engineering Consultants Inc., Chuo-ku Kiyokawa 2-13-6, Fukuoka, Japan

Abstract. In the volcanic rock fields around Hita City, 19 landslides occurred in the 2017 torrential rains in northern Kyushu, 11 of which triggered debris flows. In order to mitigate debris flows disasters caused by landslides, it is important to assess the points where landslides are most likely to occur. Therefore, topographic profiles of landslide and non-landslide slopes were calculated from digital elevation models obtained before the disaster. The results indicate that there is a topographic criterion for landslide occurrence in the relationship between the topographic position index (TPI) and the tangent Laplacian.

1 Introduction

In Japan, debris flows caused by landslides under huge precipitation amounts are common. About 200 landslides and debris flows occurred in Northern Kyushu during heavy rain at Asakura City, Toho Village, and Hita City on July 5th to 6th, 2017. The source of debris flows at Asakura city, in which the geology consists of metamorphic rocks and granitic rocks, was many small, shallow landslides with a few large landslides [1]. In contrast, large landslides were the source of debris flows at Hita and Toho districts [1], in which volcanic rocks are distributed.

The 2017 torrential rains in northern Kyushu caused landslides in 37 locations in Hita and Toho districts, where volcanic rocks are distributed, and 19 of these landslides caused debris flows. Ohta and Eguchi [2] investigated these landslides and reported that the landslides occurred at the caprock structure near the former collapse site and that the geomorphological and

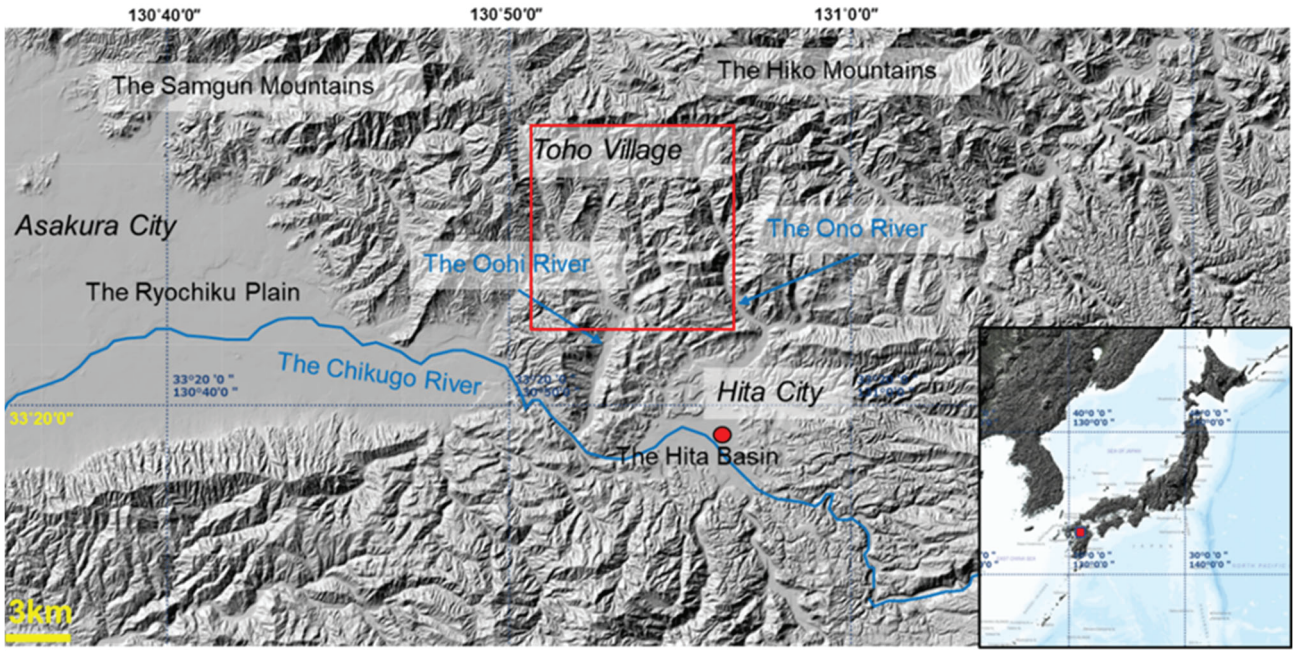

Fig. 1. Topographical map around the Hita, Toho, and Asakura area [2]. This map is based on the digital map published by the Geospatial Information Authority of Japan. The red frame shows the study area. Red point shows the Hita AMeDAS point.

* Corresponding author: takohta@yamaguchi-u.ac.jp

geological features that transitioned to debris flows were not distinct. However, it is not established the strategy to extract the slopes which have high potential to occur landslide causing debris flows.

As climate change causes torrential rains, there is concern that huge landslides accompanied by debris flows may occur simultaneously in many catchments. Therefore, it is important to clarify the criteria for the occurrence of landslide in order to mitigate debris flows hazards. In this report, a GIS analysis using a digital elevation model was used to examine the topographic criteria for landslide occurrence by comparing the topographic profiles of landslide slopes and non-landslide slopes.

2 Methods

2.1 Aerial photographic interpretation

Using aerial photographs taken after the disaster, the locations of debris flows and landslides were extracted. Aerial photographs taken before the occurrence of the disaster were used to understand the characteristics of the topography before the disaster.

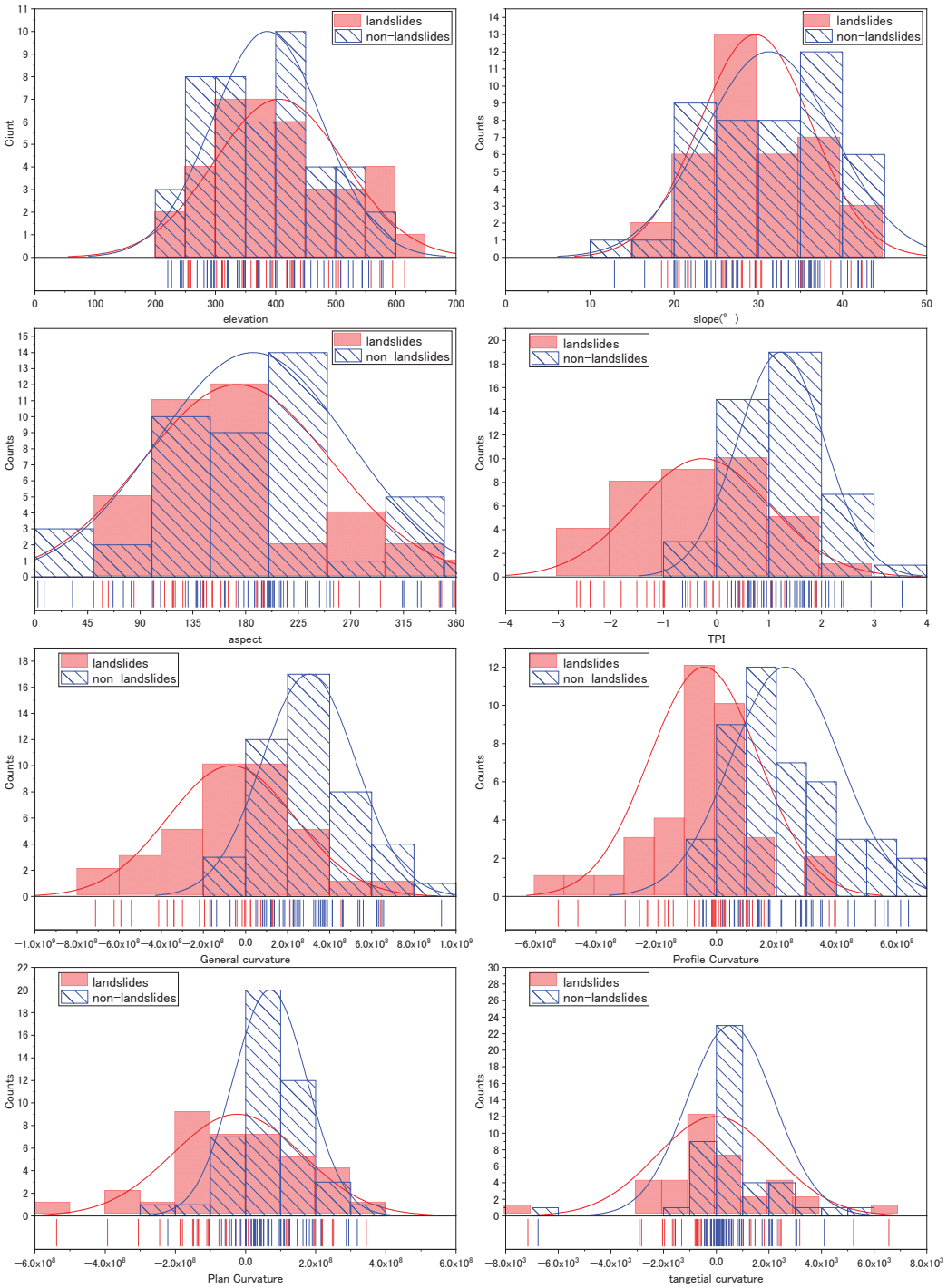

Fig. 2. Histogram of each topographic quantity.

2.2 Topographic measurement

To determine the topographic factors of landslide development that cause debris flows, topographic measurements were taken using a 10-meter mesh digital elevation model created by the Geospatial Information Authority of Japan from photogrammetric measurements in 2016, before the disaster occurred. Elevation, slope, slope direction, topographic position index (TPI) [3], general curvature, profile curvature, plan curvature [4], and tangential curvature [5] were determined for the landslide and non-landslide sites. TPI is defined as the deference between the elevation of the target point (z_0) and the average elevation ($\bar{z}$) within specific radius around it [3]. Definitional equations are shown in Equation 1 and 2 [6].

$$TPI = z_0 - \bar{z} \quad (1)$$

$$\bar{z} = \frac{1}{n_R}\sum_{i \in R} z_i \quad (2)$$

For each of the topographic quantities, the landslide area was measured at the location of the scarp occurrence, and the non-landslide area was measured at the top of the slope. The non-landslide areas were set up as follows based on Asada et al. [7] The slope unit was defined as the area bounded by the ridgelines and streamlines extracted within the primary valley catchment. The non-landslide slope top within the slope unit was defined as the convex area above the depression in the TPI map.

3 Results and discussion

From the aerial photographic interpretation, we detected 37 landslides induced by the 2017 northern Kyushu rainstorms and measured the topographic quantities in each. Forty-five non-landslide slopes adjacent to landslide were picked up and their topography measured.

3.1 Topographic measurement

Fig 2 shows the histograms of each topographic quantity. There is no remarkable difference in height, slope, or aspect between landslide and non-landslide slopes.

There is no marked difference between landslide and non-landslide slopes in elevation, slope, or aspect. The TPI for landslide slopes shows a Gaussian normal distribution centered at 0, whereas the TPI for most non-landslide slopes is positive. On landslide slopes, the general curvature and profile curvature show a Gaussian distribution with negative mean and median, while on non-landslide slopes, they have a Gaussian distribution with positive mean and median. Thus, the TPI, general curvature, and profile curvature show statistically different distributions between landslide and non-landslide slopes. For both landslide and non-landslide slopes, both plane curvature and tangential curvature are Gaussian normally distributed around 0. For both parameters, the distribution for the landslide slope is wider than that for the non-landslide slope.

3.2 Discriminant analysis

Discriminant analysis was performed on several combinations of measured topographic quantities in order to establish criteria for landslide-induced landslides. Since the statistic distribution of general curvature and profile curvature differ between landslide and non-landslide slopes, a discriminant analysis conducted using these parameters as explanatory variables. The results of the analysis are shown in Table 1, and the linear discriminant function (Eq. 3) is shown in the relationship diagram between general curvature and profile curvature, along with data for landslide and non-landslide areas (Fig. 3). The calculated error ratio was 19.22%.

$$Prof.\ cur. = -0.401 * Gen.\ cur. + 1.622 * 10^8 \quad (3)$$

Table 1. Results of discriminant analysis using general curvature and profile curvature.

	Estimated group		
	landslide	non-landslide	Total
landslide	31 83.78%	6 16.22%	37 100.00%
non-landslide	10 22.22%	35 77.78%	45 100.00%
Total	41 50.00%	41 50.00%	82 100.00%

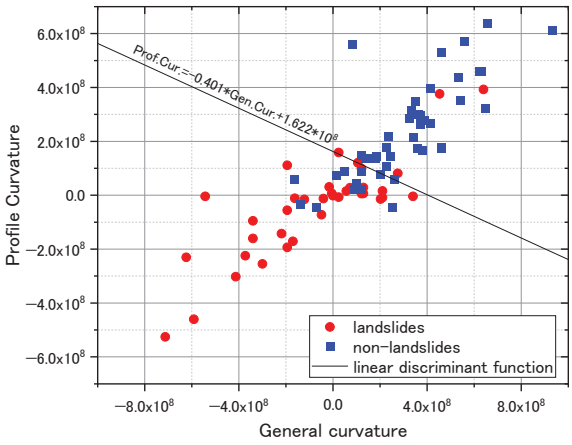

Fig. 3. Relationship diagram between general curvature and profile curvature with the linear discriminant function.

The results of the discriminant analysis using TPI and tangential curvature as explanatory variables are shown in Table 2 and Fig. 4. The linear discriminant function is as follows.

$$Tang.\ cur. = 3775 * TPI - 1822 \quad (4)$$

In this analysis, the calculated error ratio was 12.07%, the lowest value among the trials in this study. Therefore, it can be concluded that the occurrence of landslides causing debris flows can be evaluated using topographic criteria based on TPI and tangential curvature at the top of the slope. If the tangential curvature of the slope is

not less than the value of the right-hand side of Equation 4, then landslide causing debris flow are likely to occur.

Table 2. Results of discriminant analysis using TPI and tangential curvature.

	Estimated group		
	landslide	non-landslide	Total
landslide	33 89.19%	4 10.81%	37 100.00%
non-landslide	6 13.33%	39 86.67%	45 100.00%
Total	39 47.56%	43 52.44%	82 100.00%

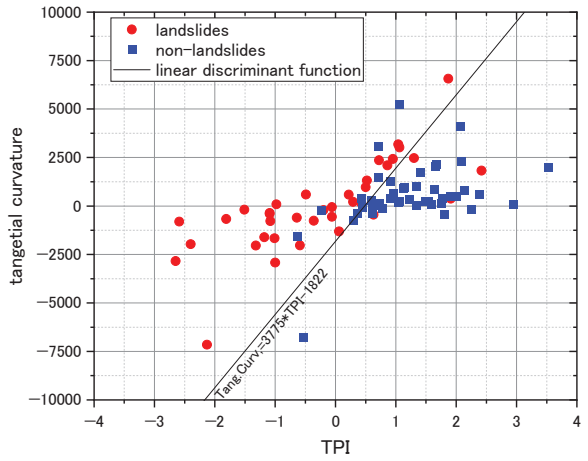

Fig. 4. Relationship diagram between general curvature and profile curvature with the linear discriminant function.

4 Conclusions

In order to establish a strategy for identifying slopes with a high potential for debris flow-causing landslide, GIS analysis using a digital elevation model was used to examine the criteria for the landslide-causing terrain. The results from these investigations suggest that;

1) There is no marked difference between landslide and non-landslide slopes in elevation, slope, or aspect.
2) TPI, general curvature, and profile curvature show statistically different distributions between landslide and non-landslide slopes.
3) From the results of the discriminant analysis using TPI and tangential curvature, which difference between landslides and non-landslides, It was not possible to obtain a linear discriminant function with good accuracy.
4) When the explanatory variables were TPI and tangent curvature, the most accurate linear discriminant function was obtained, and its error rate was 12.07%, indicating that it could discriminate with sufficient accuracy.

References

1. T. Nishimura, T. Takami and M. Matsuzawa, Outline of the situation of Landslides and Collapses that occurred in the surveyed area, Report of the 2017 Northern Kyushu Heavy Rain Disaster Research Mission, JSEG, 15-27, in Japanese (2018)
2. T. Ohta and S. Eguchi, Landslides and debris flows in volcanic rocks triggered by the 2017 Northern Kyushu heavy rain, in Proceedings of the 7th International Conference on Debris-Flow Hazards Mitigation, 10-13 June 2019, Golden, USA (2019)
3. J.C. Gallant and J.P. Wilson, Primary topographic attributes. In: Wilson, J.P., Gallant, J.C. (Eds.), Terrain Analysis: Principles and Applications. Wiley, New York, 51–85 (2000)
4. L. W. Zevenbergen and C. R. Thorne, Quantitative analysis of land sueface topography, Earth Surface Process and Landforms, **12**, 47-56 (1987)
5. L. Blaga, Apects regarding the signifiance og the curvature types and values in the studies of geomorphometry assisted by GIS, Analele Universităţii din Oradea, Seria Geografie, **XXII**, 327-337 (2012)
6. J. De Reu, J. Bourgeois, M. Bats, A. Zwertvaegher, V. Gelorini, P. De Smedt, W. Chu, M. Antrop, P. De Maeyer, P. Finke, M. Vanv Meirvenne, J Verniers and P. Crombé, Application of the topographic position index to heterogeneous landscapes, **186**, 39-49 (2013)
7. H. Asada, T. Minagawa, A. Koyama and H. Ishiyanagi, Factor analysis of surface collapse on slopes caused by the July 2017 Northern Kyushu Heavy Rain, Ecol. Civil Eng., **23**, 185-196 (2020)